Published in final edited form as:
Biomacromolecules. 2012 March 12; 13(3): 826–832. doi:10.1021/bm201731e.

Silk Self-Assembly Mechanisms and Control-From Thermodynamics to Kinetics

Qiang Lu[a,b,c,*], **Hesun Zhu**[d], **Cencen Zhang**[a], **Feng Zhang**[c], **Bing Zhang**[e], and **David L. Kaplan**[b,*]

[a]National Engineering Laboratory for Modern Silk, College of Textile and Clothing Engineering, Soochow University, Suzhou 215123, People's Republic of China

[b]Department of Biomedical Engineering, Tufts University, Medford, MA 02155, USA

[c]Jiangsu Province Key Laboratory of Stem Cell Research, Soochow University, Suzhou 215006, People's Republic of China

[d]Research Center of Materials Science, Beijing Institute of Technology, Beijing, 100081, People's Republic of China

[e]School of Chemical Engineering, Zhengzhou University, Zhengzhou 450001, People's Republic of China

Abstract

Silkworms and spiders generate fibres that exhibit high strength and extensibility. The underlying mechanisms involved in processing silk proteins into fiber form remain incompletely understood, resulting in the failure to fully recapitulate the remarkable properties of native fibers in vitro from regenerated silk solutions. In the present study, the extensibility and high strength of regenerated silks were achieved by mimicking the natural spinning process. Conformational transitions inside micelles, followed by aggregation of micelles and their stabilization as they relate to the metastable structure of silk are described. Subsequently, the mechanisms to control the formation of nanofibrous structures were elucidated. The results clarify that the self-assembly of silk in aqueous solution is a thermodynamically driven process where kinetics also play a key role. Four key factors, molecular mobility, charge, hydrophilic interactions and concentration underlie the process. Adjusting these factors can balance nanostructure and conformational composition, and be used to achieve silk-based materials with properties comparable to native fibers. These mechanisms suggest new directions to design silk-based multifunctional materials.

Keywords

Silk Self-Assembly; Biomaterials; Kinetics; Nanostructure

1. Introduction

Silk, one of the toughest and most versatile materials known, is a biological protein fibre with exceptional mechanical properties and biocompatibility. In recent years, silk-based materials have been transformed into high-technology uses [1], with a promising future in tissue engineering, [2, 3] drug release systems, [4, 5] and optical applications. [6, 7] In addition, expanding insight has been attained into silk production, nanostructure formation, biological

Corresponding authors: David L. Kaplan, Fax: (617)627-3231; david.kaplan@tufts.edu. Qiang Lu, Tel: (+86)-512-67061649; Lvqiang78@suda.edu.cn.

properties and mechanical properties. [8–11] Silk features exceptional mechanical properties with high elastic modulus, high tensile strength and great extensibility,[12] but silk-based membranes and films still lack mechanical robustness though similar β-sheet structure with natural silk fibers is achieved in these materials.[13] Recent study indicates that the excellent mechanical properties of silk fibroin are also related to the nanostructures of β-sheet crystal that are built up through self-assembly process *in vivo*.[12] However, the recapitulation of native silk fibroin dope and fiber properties in vitro from reconstituted silk solutions remains a challenge, particularly because controlled self-assembly of macromolecular components at the nanoscale is required. [12–15]

We and others have reported mechanisms for silk processing, including the formation of globular nanoscale features as a key step in the formation of silk fibers [16]. Several ameliorated models were proposed to gain further insight into the aggregation process of silk. [17, 18] However, compared to the natural silk forming process, the control of nanofiber formation remains unclear, as does, how silk fibroin assemblies maintain stability in a concentrated silk dope without irreversible precipitation or crystallization, yet is still able to rapidly convert from random coil and/or helix to β-sheet during spinning [1]. These unknowns make reconstitution of silk solutions into materials with properties comparable to the native state problematic.

2. Materials and methods

2.1 Silk solution and films

Silk solution and films with silk I structure were produced as described. [19, 20] Cocoons were boiled for 20 min in an aqueous solution of 0.02 M Na_2CO_3 and then rinsed thoroughly with distilled water to extract the sericin proteins. After drying, 13.5 g extracted silk fibroin was dissolved in 50 ml of LiBr solution (9.3 M) at 60°C for 4 h, yielding a 20% (w/v) solution. This solution was dialyzed against distilled water using Slide-a-Lyzer dialysis cassettes (Pierce, molecular weight cut-off 3,500) for 72 h to remove the salt. The solution was optically clear after dialysis and was centrifuged to remove the small amount of silk aggregates that formed during the process. The final concentration of aqueous silk solution was ~7 wt%, determined by weighing the remaining solid after drying. The silk fibroin solution was then diluted to 6 wt% with water. Since silk fibroin is slowly concentrated to above 30wt% and transfers to silk I structure before spinning in vivo, silk films mainly composed of silk I structure were formed with a slower drying time of above 5 days according to our previous procedures.[19] The films were hydrated in distilled water for approximately 30 min before clamping and then stretched to 200% of their original length at a crosshead speed of 5 mm min^{-1} using an Instron 3366 testing frame (Instron, Norwood, MA), resulting in the formation of silk II structure.

2.2 Slow concentrated process of silk fibroin

The fresh silk fibroin solutions were cast onto polystyrene Petri dish surfaces (diameter 100 mm) and then control the drying rates with lids with different numbers of the holes (thus air exchange rate), making silk fibroin dry at day 6. At designated time points (0, 3, 5 and 6 days), part of silk fibroin solution was removed to measure the changes of nanostructures and secondary structures. The concentrations of silk fibroin were 6 wt%, 12 wt% and 20 wt % when concentrated for 0, 3 and 5 days, respectively.

2.3 Silk sample preparation

For FTIR, DSC and SEM experiments, all samples were flash frozen and dried in liquid nitrogen to preserve original structures as accurately as possible based on our previous

studies.[21, 22] For AFM experiments, silk solutions were diluted to below 0.1 wt% to avoid masking the original morphology by multilayers of silk.

The microstructures of silk samples were studied with Zeiss Supra 55 VP SEM (Oberkochen, Germany), and AFM (Veeco, Nanoscope V, NY). In AFM measurement, 2 μl of the diluted SF solution was dropped onto freshly cleaved 4×4 mm^2 mica surfaces. The morphology of silk fibroin in water were observed by AFM in air. A 225 μm long silicon cantilever with a spring constant of 3 Nm^{-1} was used in tapping mode at 0.5–1 Hz scan rate. Then the freeze-dried samples were fractured in liquid nitrogen to avoid deformation and sputter-coated with platinum and examined using a Zeiss Supra 55 VP SEM.

The secondary structures of silk samples were studied with Jasco FTIR-6200 spectrometer (Japan), and Q100 DSC (TA Instruments, New Castle, DE) according to our previous methods.[19, 23] In FTIR study, 32 scans were coded for each measurement at a resolution of 4 cm^{-1}, with the wave number ranging from 400 to 4000 cm^{-1}. Then the thermal properties of the samples were measured in a TA instrument Q100 DSC under a dry nitrogen gas flow of 50 ml min^{-1}. Temperature-modulated differential scanning calorimetry (TMDSC) measurements were performed using a TA instrument Q100 equipped with a refrigerated cooling system. The samples were heated at 2°C min^{-1} with a modulation period of 60s and a temperature amplitude of 0.318°C.

3. Results and Discussion

In the natural process, a silk fibroin solution dope or hydrogel forms in the gland before spinning. The dope is composed of silk chains in silk I (organized but not beta sheet) structures, considered to be a necessary intermediate for the pre-organization or prealignment of silk fibroin molecules. [24] Upon spinning, the metastable silk I structure transitions into the stable silk II (beta sheet) structure. Unfortunately, the reproduction of silk I in vitro from regenerated silk fibroin solution remains challenging. Although recent studies confirmed the formation of nanofibrils in natural silk processing, [25] the process for nanofibril formation remains to be clarified. By experimentally simulating aspects of the natural silk assembly process, our recent investigations revealed that silk films composed of silk I could be prepared by the slow drying of silk solutions at room temperature.[19] Once the hydrated silk fibroin films were stretched, flexibility in the dry state was achieved following the conformational transition from silk I into silk II (Fig 1A). With a decrease in the diameter of nanofilaments, the nanofilaments in the films aligned after stretching (Fig 1A(a and b)). The orientated nanofilaments consisted of nanoparticles about 20 nm in diameter, similar to the nanofibrils in natural silk. [25] Considering the similarity between the silk fibroin films in our prior study and natural silk fibers, including conformational changes, nanostructure and mechanical properties, the silk fibroin films and the process used to generate these films were determined to be a suitable model to study the controlled nanoscale self-assembly of silk fibroin chains.

Therefore, we examined the microstructure and conformational changes of silk fibroin during the very slow drying process. Closer examination of the microstructure of silk fibroin by scanning electron microscopy (SEM) and atomic force microscopy (AFM) indicated that the silk first self-assembled into micelles, similar to our previous observations, [26] and then the micelles aggregated into nanofilaments rather than globules (Fig 2A) in concentrated silk solutions.

The pattern of hydrophobic and hydrophilic domains in the silk fibroin heavy chain include larger hydrophilic domains at the chain ends, smaller hydrophilic internal domains and large internal hydrophobic domains.[26] Based on thermodynamics, silk fibroin molecules act as

hydrophilic-hydrophobic-hydrophilic polymers, with the formation of micellar structures in water in which the larger terminal hydrophilic blocks define the outer edges of the micelles while the large hydrophobic blocks and small hydrophilic blocks are present inside the micelles.[16–18] However, the structural and conformational changes of the micelles in the assembly process are unclear, making it challenging to regulate nanostructure formation. The large hydrophobic blocks and small hydrophilic blocks are assumed to be initially distributed randomly inside the micelles. Then the hydrophobic blocks gradually arrange to form more regular structures, and eventually silk I like-structures or silk II structures, while the small hydrophilic blocks may move to the surface of the micelles to interact with water by chain folding, reducing the free energy of the silk fibroin-water system. Therefore, this initial structure is thermodynamically unstable, suggesting the possibility of rearrangement of micellar structures in water (Fig. 3). The interpretation of this behavior is supported by our examination of the structural and conformational changes during the very slow drying process. Although silk fibroin maintained random conformation even in concentrated aqueous solutions (>50 wt%), a crystallization peak first appeared at 214°C, and then decreased to 210°C following slow drying (Fig 1B). Crystallization gradually became easier during the process, indicating the increase of structural regularity within the micelles and the formation of metastable intermediate states that facilitated crystallization upon spinning or stretching. This behaviour suggests a dynamic process, also determined by the rate of chain folding. Changing hydrophilic/hydrophobic interactions and molecular motility would control the phase behavior during the silk self-assembly process. If hydrophilic interaction and molecular mobility increased in silk fibroin solution, the rate of chain folding would increase to get stabler structure more quickly. Several recent studies have confirmed this assumption. Higher temperature and stronger hydrogen bonding accelerate the rate of chain folding rate, reducing the time for transitions from random to crystal structure. [21, 27]

Besides the insight of conformational transitions, silk self-assembly from micelles to nanofibrils can also be clarified. Recent studies revealed that the exceptional strength of silkworm and spider silks might arise from the arrangement of regular nanostructures [12] with the nanofibrils as the main structural features of silks with a diameter of about 20 nm and consisting of the organized micelles.[25] Unfortunately, the natural self-assembly process from micelles to nanofibrils has eluded experimental insight. The aggregation mechanism of micelles was therefore also investigated in the present study. The nanostructure changes of silk fibroin during the slow drying process indicated that the micelles easily aggregated into nanofibrils rather than larger globules in the absence of other additions in concentrated silk solutions, following the increase of hydrophilic interactions between silk fibroin and bound water. AFM images of silk fibroin derived from the middle part of the gland of the fifth instar (L5) *Bombyx mori* silkworm larvae also showed that nanofibrous structures formed in the gland before spinning (Fig 2A(i)). This result suggests a new model in which negative charges on the silk fibroin chains, and silk concentration, are important factors in controlling micelle aggregation. The isoelectric point of silk fibroin is about 4.2, so silk fibroin contains negative surface charge in neutral aqueous solution due to the acidic charged groups. In dilute silk solutions, the repulsive forces between the negative charges results in the formation of stable micelles in solution. In concentrated silk solutions, in order to reduce repulsive forces, fibril formation from the micelles is the preferred assembly path since an approaching micelle suffers repulsive force from only one micelle during fibril formation in contrast to larger repulsive forces from multiple micelles in the case of globule formation (Fig 4A). This mechanism is supported by the different structures of silk gels derived from diluted and concentrated silk solutions, respectively. Silk maintains micellar morphology when diluted silk solutions (1 wt%) are transformed into hydrogels after 18 days at room temperature, however, in contrast they assemble into fibrils if the hydrogel is prepared from concentrated silk solutions (20 wt%) (Fig 4B(a) and (b)). During the process in which silk is transformed from different intermediate structures to silk II, silk fibroin maintains micellar

structures, indicating that these early transformations occur mainly inside the micelles. The effect of negative charge on controlling micellar aggregation was further confirmed by our recent electrogelation studies,[20, 22] where under electric fields the repulsive forces of the negative charges were shielded and micelles aggregated to form globules rather than nanofibrils (Fig 4B(c)). This micellar aggregation behavior induced by electrolysis-induced pH changes confirmed the transitions. Silk fibroin solution containing uniform sized micelles were prepared by changing silk fibroin concentrations. In neutral solution, micelles were stably maintained at 4°C for 6 hours because of the negative charge repulsion. After the pH decreased to about the isoelectric point (~4.2), the micelles aggregated to larger globules following the shielding of the negative repulsive forces under the same conditions (Fig 5).

As an important part of the silk fibroin self-assembly mechanism, critical factors that stabilize the metastable state of silk fibroin were also clarified. In nature, the process of avoiding crystallization of the protein until the final step of silk spinning into fibers is critical to achieve outstanding mechanical properties, while also being essential to the survival of the organism. To clarify this step in the process, we determined structural features of the silk fibroin before and after crystallization. The silk fibroin was characterized by temperature-modulated DSC method according to our previous study [19], and the results indicated that most hydrophilic silk-bound water interactions were destroyed by the formation of the silk II structure but were maintained after silk I formation (Fig. 6A and B). These hydrophilic interactions may be critical in suppressing premature crystallization in natural silk processing. Silk II is β-sheet crystal structure while silk I is β-turn structure. Compared to silk I, silk II is stabler structure of silk fibroin. Based on thermodynamic mechanisms, silk fibroin gradually transformed from random coil structures to the silk II structure rather than silk I structure. However, in order to form the silk II structure, silk fibroin molecules have to overcome the energy barrier resulting from the hydrophilic interactions. When the molecular mobility of silk fibroin in the intermediate stage is sufficient to overcome this barrier, silk fibroin will transform into the silk II structure. Silk fibroin in the intermediate stages transforms into silk I structures because this energy barrier is much lower than for silk II. Further experiments were designed to confirm this view. A concentrated silk solution (20 wt%) was placed at room temperature and kept in the solution state for 6 days. During this time, silk fibroin gradually rearranged and finally formed hydrogels. Through freeze-drying the silk fibroin solution that was rearranged for different time frames, the silk fibroin materials were prepared with different levels of hydrophilic interactions (Fig 6C). Following increased time for rearrangement, hydrophilic interactions between the silk and bound water increased. At the same time, the intermediate metastable structure also increased slightly. These silk fibroin systems were then heated above the crystallization temperature. FTIR analysis of the heated silk fibroins showed that less β-sheet structure formed with stronger hydrophilic interactions, confirming the inhibiting effect of hydrophilic interactions on silk II crystallization (Fig 6D). These mechanisms were also confirmed by adding glycerol to the silk solution to increase hydrophilic interactions (hydrogen bonds), where the complete hydrogelation of a 20 wt% silk fibroin solution increased from 5±1 days to 10±2 days at room temperature following the addition of the glycerol (glycerol content 20 wt% in the dried silk fibroin). Therefore, by controlling hydrophilic interactions and silk chain mobility, different silk fibroin-based materials composed of silk I rather than silk II were prepared, leading to an extended range of material properties. [4, 19, 21, 28]

As indicated, silk self-assembly in aqueous solution has two different but correlative aspects, conformational transitions and nanostructure assembly. Self-assembly is not only a thermodynamic process in which silk fibroin chains form stable solid-state silk II crystals, but also a kinetic process that involves four key factors including molecular mobility,

hydrophilic/hydrophobic interactions, charge and concentration (water content). The synergistic effect of these factors results in conformational changes and the formation of nanostructures, making it difficult to elucidate self-assembly mechanisms.[29–31] For example, silk fibroin micelles can retain a homogeneous size in dilute solution (0.1 wt% silk in water) for several days at 4°C, while the chains are inclined to aggregate into larger globules at 60°C since higher molecular mobility overcomes the repulsive forces of the negative charges. This self-assembly mechanism is elucidated in our present model by including distilled water as solvent to avoid the complexity of salt interactions. By controlling the four key factors above, in different stages of the process, a balance between nanostructure and conformational composition was achieved to control the properties of silk materials. Our previous self-assembly mechanism revealed micellar structures, however many aspects of the process remained undefined. With the mechanism described here, gaps in understanding how to regenerate silk fibroin fibers and to stabilize the metastable state of silk are clarified by considering the self-assembly of silk fibroin not only as a thermodynamic process but also a kinetic process.

The mechanisms illustrate how to control the nanostructure and crystallization of silk under mild (aqueous, ambient) conditions. Silk fibroin micelles assemble into nanofibrils by control of the negative charges and concentration, following the increase of hydrophilic interactions since the micelles are connected by the interactions. Subsequently, stronger hydrophilic interactions as well as decreased molecular mobility in concentrated solution restrains premature crystallization from the metastable state. After physical spinning or stretching, the nanofibrils elongate and align, allowing the structural transition to the insoluble crystalline silk II structure to establish the basis for the high-strength silk fibres. More importantly, the elucidation of the mechanisms also implies that the nanostructures and conformations can be controlled and stabilized at different stages by adjusting molecular mobility, charge, hydrophilic interactions and concentration, providing new ways to design desired nanostructures and related features of silk. These control points indicate how to regulate the formation of silk biomaterials with targeted properties.

4. Conclusions

In this study, the self-assembly process of silk fibroin in aqueous solutions is elucidated, indicating that silk fibroin assembles from microspheres to nanofilaments. The self-assembly of silk fibroin is not only a thermodynamic process but also a kinetic process, which could be controlled by adjusting molecular mobility, charge, hydrophilic interactions and concentration. Based on the mechanism, it is feasible to design silk fibroin materials with desired properties.

Acknowledgments

We thank the Priority Academic Program Development of Jiangsu Higher Education Institutions (PAPD) and Ph.D. Programs Foundation of Ministry of Education of China(201032011200009) for support of this work. We also thank the NIH, the AFOSR, National Natural Science Foundation of China (21174097), and the Key Natural Science Foundation of the Jiangsu Higher Education Institutions of China(11KGA430002) for support of this work.

References

1. Omenetto FG, Kaplan DL. Science. 2010; 329:528–531. [PubMed: 20671180]
2. Patra C, Talukdar S, Novoyatleva T, Velagala SR, Muhlfeld C, Kundu B, Kundu SC, Engel FB. Biomaterials. 2012; 33:2673–2680. [PubMed: 22240510]
3. Lu Q, Wang XL, Lu SZ, Li MZ, Kaplan DL, Zhu HS. Biomaterials. 2011; 32:1059–1067. [PubMed: 20970185]
4. Hofer M, Winter G, Myschik J. Biomaterials. 2012; 33:1554–1562. [PubMed: 22079006]

5. Lammel AS, Hu X, Park SH, Kaplan DL, Scheibel TR. Biomaterials. 2010; 31:4583–4591. [PubMed: 20219241]
6. Tsioris K, Tilburey GE, Murphy AR, Domachuk P, Kaplan DL, Omenetto FG. Adv Funct Mater. 2010; 20:1083–1089.
7. Amsden JJ, Domachuk P, Gopinath A, White RD, Negro LD, Kaplan DL, Omentto FG. Adv Mater. 2010; 22:1746–1749. [PubMed: 20496408]
8. Yucel T, Cebe P, Kaplan DL. Adv Funct Mater. 2011; 21:779–785.
9. Fu C, Porter D, Chen X, Vollrath F, Shao ZZ. Adv Funct Mater. 2011; 21:729–737.
10. Shao ZZ, Vollrath F. Nature. 2002; 418:741–471. [PubMed: 12181556]
11. Jiang CY, Wang XY, Gunawidjaja R, Lin YH, Gupta MK, Kaplan DL, Naik RR, Tsukruk VV. Adv Funct Mater. 2007; 17:2229–2237.
12. Keten S, Xu Z, Ihle B, Buehler MJ. Nat Mater. 2010; 9:359–367. [PubMed: 20228820]
13. Kharlampieva E, Kozlovskaya V, Wallet B, Shevchenko VV, Naik RR, Vaia R, Kaplan DL, Tsukruk VV. ACS Nano. 2010; 4:7053–7063. [PubMed: 21090657]
14. Holland C, Terry AE, Porter D, Vollrath F. Polymer. 2007; 48:3388–3392.
15. Holland C, Terry AE, Porte D, Vollrath F. Nat Mater. 2006; 5:870–874. [PubMed: 17057700]
16. Jin HJ, Kaplan DL. Nature. 2003; 424:1057–1061. [PubMed: 12944968]
17. Rammensee S, Slotta U, Scheibel T, Bausch AR. Proc Natl Acad Sci USA. 2008; 105:6590–6595. [PubMed: 18445655]
18. Martel A, Burghammer M, Davies RJ, Cola ED, Vendrely C, Riekel C. J Am Chem Soc. 2008; 130:17070–17074. [PubMed: 19053481]
19. Lu Q, Hu X, Wang X, Kluge JA, Lu S, Cebe P, Kaplan DL. Acta Biomater. 2010; 6:1380–1387. [PubMed: 19874919]
20. Lu Q, Huang YL, Li MZ, Zuo BQ, Lu SZ, Wang JN, Zhu HS, Kaplan DL. Acta Biomater. 2011; 7:2394–2400. [PubMed: 21345387]
21. Lu SZ, Wang XQ, Lu Q, Zhang XH, Kluge JA, Uppal N, Omenetto F, Kaplan DL. Biomacromolecules. 2010; 11:143–150. [PubMed: 19919091]
22. Leisk GG, Lo T, Yucel T, Lu Q, Kaplan DL. Adv Mater. 2010; 22:711–715. [PubMed: 20217775]
23. Hu X, Kaplan DL, Cebe P. Macromolecules. 2008; 41:3939–3948.
24. Kratky O, Schauenstein E, Sekora A. Nature. 1950; 165:319–320.
25. Du N, Yang Z, Liu XY, Li Y, Xu HY. Adv Funct Mater. 2011; 21:772–778.
26. Zhou CZ, Confalonieri F, Medina N, Zivanovic Y, Esnault C, Yang T, Jacquet M, Janin J, Duguet M, Perasso R, Li ZG. Nucleic Acids Res. 2002; 28:2413–2419. [PubMed: 10871375]
27. Lv Q, Cao CB, Zhang Y, Ma X, Zhu HS. J Appl Polym Sci. 2005; 96:2168–2173.
28. Jin HJ, Park J, Karageorgiou V, Kim U, Valluzzi R, Cebe P, Kaplan DL. Adv Funct Mater. 2005; 15:1241–1247.
29. Inoue SI, Tsuda HT, Tanaka T, Kobayashi M, Magoshi Y, Magoshi J. Nano Lett. 2003; 3:1329–1332.
30. Trancik JE, Czernuszka JT, Bell FI, Viney C. Polymer. 2006; 47:5633–5642.
31. Shulha H, Wong Po Foo C, Kaplan DL, Tsukruk VV. Polymer. 2006; 47:5821–5830.

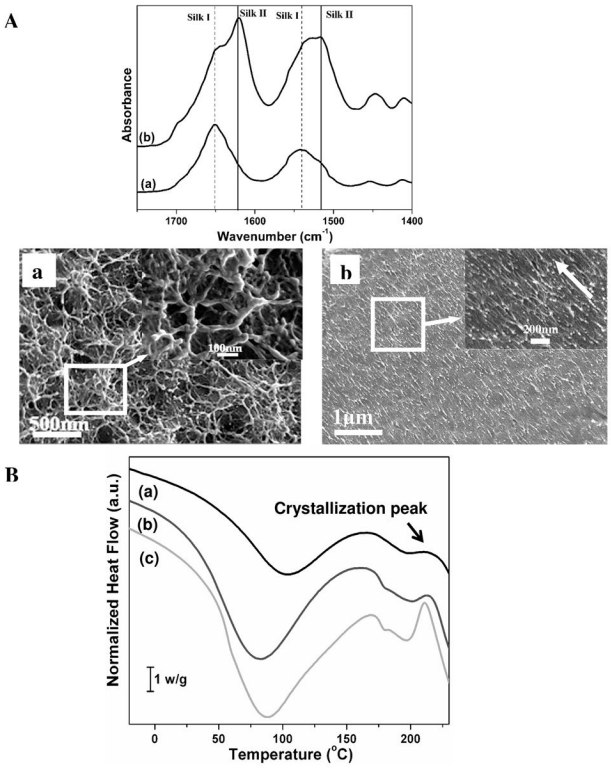

Figure 1.

A) FTIR and SEM results from silk films prepared by very slow drying (a) and then stretching the films 200%; B) DSC curves for silk materials derived from concentrated silk solutions in very slow drying process. (a) original silk solution, silk concentration 6 wt%; (b) silk solution was concentrated for 3 days, silk concentration about 12 wt%; and then (c) 5 days, silk concentration about 20 wt%. The intensity of the crystallization peak increased and shifted to a lower temperature, indicating the increase of structural regularity of the intermediate structures in the slow drying process.

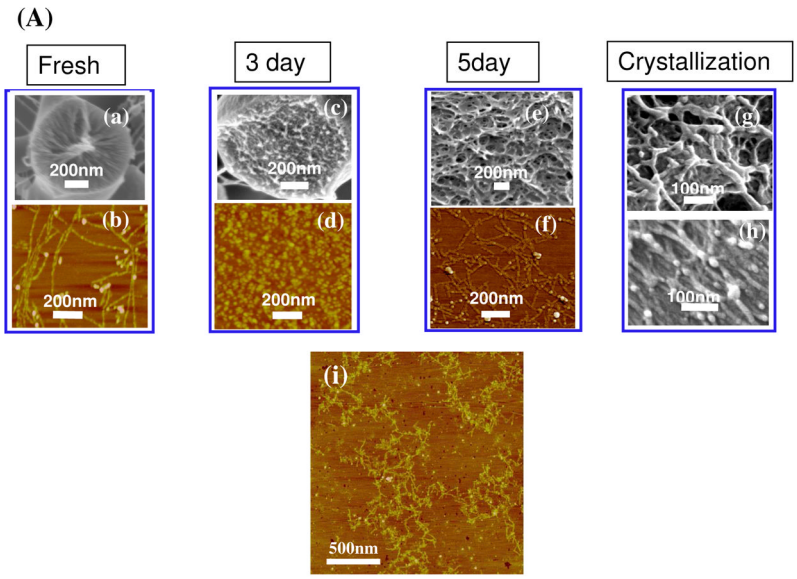

Figure 2.

Self-assembly including micelle formation, further rearrangement of micelles, nanofilament formation and crystallization of silk fibroin in very slow drying process (A). Fresh silk fibroins gradually self-assemble from molecular chains (a, b) to micelles at day 3 (c, d), nanofilaments at day 5 (e, f), and then silk I formation in films at day 6 (g) and finally silk II formation after stretching the films 200% (h). Nanofilaments also form in silk dope from the middle gland of the L5 *B. mori* silkworm larvae (i). ((a, c, e, h) SEM images, (b, d, f, i) AFM images)

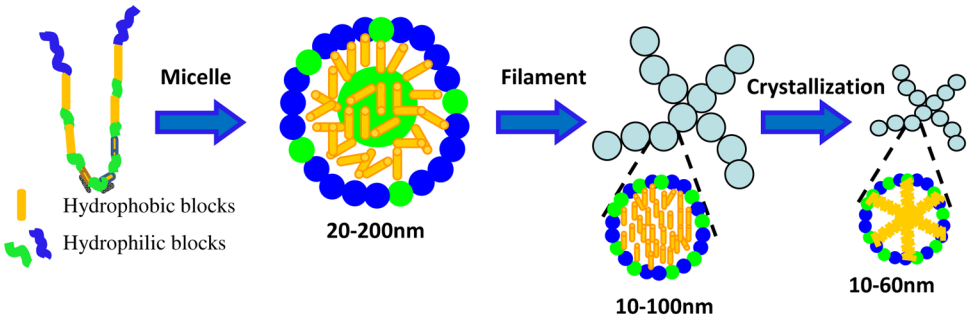

Figure 3.
Self-assembly model including micelle formation, further rearrangement of micelles, nanofilament formation and crystallization of silk fibroin

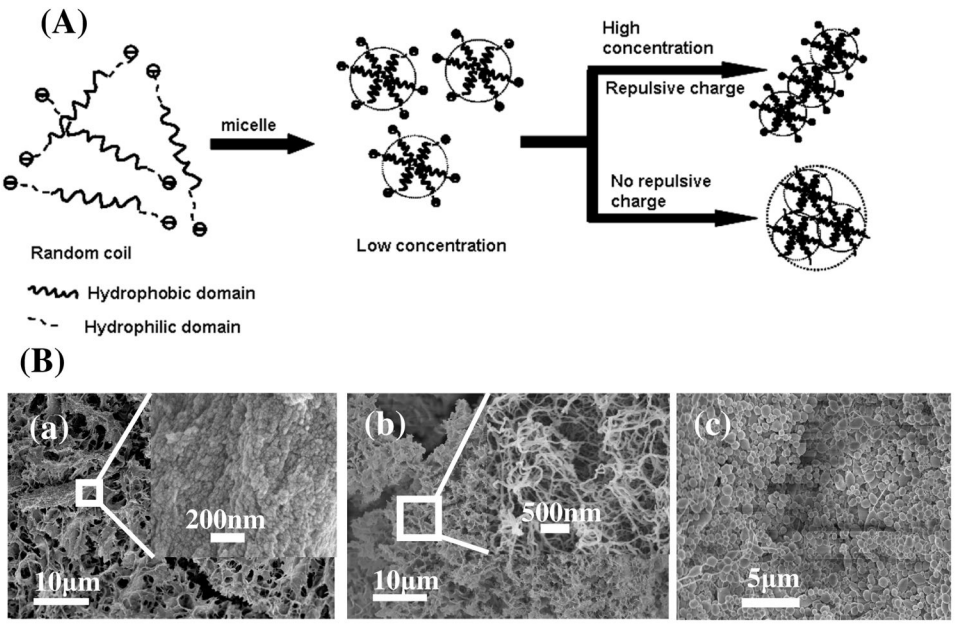

Figure 4.

(A) Model of silk micelle assembly controlled by silk concentration and the negative charges on the amino acid side chains. (B) SEM images of different hydrogels derived from silk solution with low concentration (1 wt%) (a), high concentration (20 wt%) (b) and electrically mediated from silk fibroin (c).

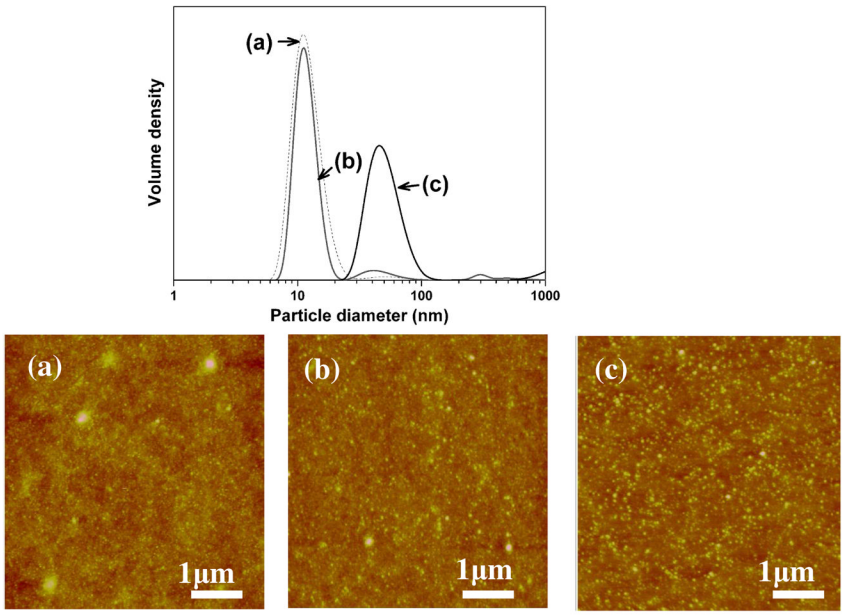

Figure 5.
Size changes of silk micelles in dilute solution (0.15 wt%) following the shielding of negative charges of repulsion. Dilute silk solution (a) maintained small micelles structure at neutral solution (b) while assemble larger globules at about the isoelectric point (c) when stored at 4°C for 6h.

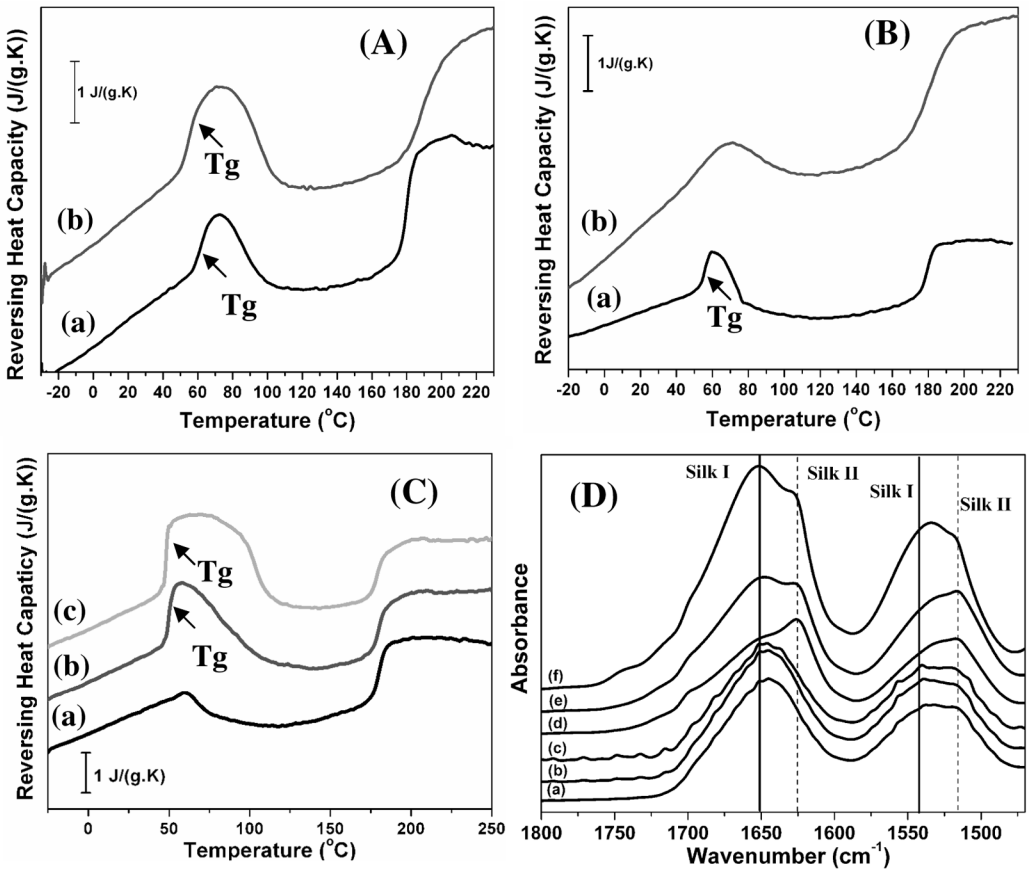

Figure 6.

TMDSC curves for silk fibroin before and after crystallization and hydrophilic interaction effects on silk II crystallization. (A) Heat capacity changes (ΔCp) at Tg before (a) and after silk I formation (b). The ΔCp changed from 0.18 J/(g.K) to 0.19 J/(g.K). (B) Heat capacity changes (ΔCp) at Tg before (a) and after silk II formation (b). The ΔCp changed from 0.31 J/(g.K) to 0.06 J/(g.K). (C) TMDSC curves for silk fibroin derived from concentrated silk solutions (20 wt%) that self-assembled for 0 day (a), 2 days (b) and 4 days (c) at room temperature, following the increase of heat capacity (ΔCp) from 0 J/(g.K) to 0.43 and 0.57 J/(g.K), respectively. (D) FTIR spectra for silk fibroin derived from concentrated silk solutions (20 wt%) that self-assembled for 0 day (a), 2 days (b) and 4 days (c) at room temperature, and then heat treatment with DSC (d, e, f), respectively. The samples were heated at 2°C min^{-1} from −30 to 230°C to avoid degradation.